



Merging of ozone profiles from SCIAMACHY, OMPS and SAGE II observations to study stratospheric ozone changes

Carlo Arosio¹, Alexei Rozanov¹, Elizaveta Malinina¹, Mark Weber¹, and John P. Burrows¹

¹Institute of Environmental Physics, University of Bremen, Bremen

Correspondence to: carloarosio@iup.physik.uni-bremen.de

Abstract. This paper presents vertically and zonally resolved merged ozone time series from limb measurements of the SCanning Imaging Absorption spectroMeter for Atmospheric CHartographY (SCIAMACHY) and the Ozone Mapping and Profiler Suite (OMPS). In addition, we present the merging of the latter two data sets with zonally averaged profiles from the Stratospheric Aerosol and Gas Experiment (SAGE) II. The retrieval of ozone profiles from SCIAMACHY and OMPS is performed at the University of Bremen. Within the merging procedure of these two time series we use data from the Microwave Limb Sounder (MLS) as a transfer function and we follow two approaches: (1) a standard method involving the calculation of deseasonalized anomalies and (2) a plain-debiasing approach, generally not considered in previous similar studies, which preserves the seasonal cycles of each instrument. We find a good correlation and no significant drifts between the merged and MLS time series. Using the merged data set, we apply a multivariate regression analysis to study ozone changes over the 2003–2018 period in the 20–50 km vertical range. Exploiting the high horizontal sampling of the instruments, we investigate not only the zonally averaged field but also the longitudinally resolved long-term ozone variations, finding a remarkable variability, especially at mid- and high-latitudes. Significant positive linear trends of about 2–4 % per decade were identified in the upper stratosphere between 38 and 45 km at mid-latitudes. This is in agreement with the predicted recovery of upper stratospheric ozone, which is attributed both to the adoption of measures to limit the release of halogen-containing ozone-depleting substances included in the Montreal protocol and to the increasing concentration of greenhouse gases. In the tropical stratosphere below 25 km negative but non-significant trends were found. We compare our results with similar previous studies and with short-term trends calculated over the SCIAMACHY period: while a general agreement is found, some discrepancies are seen in the tropical mid-stratosphere. Regarding the merging of SAGE II with SCIAMACHY and OMPS, zonal mean anomalies are taken into consideration and ozone trends after and before 1997 are shown. Negative trends above 30 km are found for the 1985–1997 period, with a peak of -6 % per decade at mid-latitudes, in agreement with previous studies. The increase of ozone concentration in the upper stratosphere is confirmed considering the 1998–2018 period. Trends in the middle and lower tropical stratosphere are found to be non-significant.

1 Introduction

The continuous monitoring of the stratospheric ozone layer is considered by the scientific community an important and key activity, required to assess the impact of anthropogenic and natural processes. Variations of ozone concentration in time at



different altitudes and latitudes respond to and are intertwined with several dynamical and chemistry-related processes in the atmosphere.

Two important chemical forcings that have influenced globally the amount and distribution of stratospheric ozone over the last decades are the loadings of the so-called halogen-containing ozone-depleting substances (ODSs), that is halogen source gases released by human activities as chlorofluorocarbons (CFCs), and of greenhouse gases (GHGs). The adoption of the Montreal Protocol and its amendments regulated the industrial production of chlorine and bromine compounds: species like the CFCs have been banned during '90 in most countries, leading to a decrease of their concentration in the stratosphere starting from the beginning of the century (WMO, 2014). This decrease is expected to lead to a recovery of the ozone layer globally and in particular over the Antarctic region, affected by the spring-time ozone hole. On the other hand, the increasing concentration of GHGs as CO₂ and CH₄ in the troposphere, is causing a cooling of the stratosphere, through radiative transfer feedbacks. This cooling leads to ozone increases due to the reactions R1 and R2 :



which have a strong temperature dependence (Groves et al., 1978; Groves and Tuck, 1979). Cooling the stratosphere results in increased production and slower loss of ozone: a so called super recovery is thus expected (WMO, 2014). Models suggest that the combined effect of decreasing ODSs and increasing GHGs is going to lead to an increase in stratospheric ozone in the current and in the next decades, depending on the chosen scenario of anthropogenic emissions and on the actual decrease of ODSs (Waugh et al., 2009; Morgenstern et al., 2018).

Another important species determining stratospheric ozone concentration belongs to the NO_x family (NO, NO₂). The increasing tropospheric emissions of N₂O or its longer residence time is causing a rise of NO concentration in the stratosphere and a more efficient ozone destruction via the temperature-dependent NO_x catalytic cycle. N₂O is a long-life GHG and it is expected to play a central role in the ozone recovery process over the next decades (Ravishankara et al., 2009) and it is rapidly becoming the most important ODS emitted by human activities (Portmann et al., 2012). In addition, increasing emissions of CH₄ at the surface result in increasing CH₄ in the stratosphere and thus also of HO_x (H, OH, HO₂). However the overall impact of increasing CH₄ is complex in the stratosphere: the ozone depletion by the HO_x catalytic destruction cycles occurs in the upper stratosphere, whereas the catalytic production of ozone is favoured by increasing HO_x and sufficient NO_x in the lower stratosphere.

Changes in stratospheric dynamics also affect the latitudinal and altitudinal distributions of ozone. In particular, the speed of the tropical upwelling, i.e. the strength of the upward branch of the Brewer–Dobson circulation (BDC), is directly related to changes in the ozone distribution in the tropical lower and middle stratosphere. An acceleration of the stratospheric mean mass transport has been predicted by several model studies (Garcia and Randel, 2008), but strong inter-annual variations prevents a significant recognition of this trend from observations. From monthly up to decadal time scale, ozone concentration is also influenced by many well known phenomena such as the 11-year solar activity cycle and solar proton events, the Quasi-Biennial Oscillation (QBO), El Niño Southern oscillation (ENSO), and volcanic eruptions.



Interactions of all these chemistry- and dynamics-related contributions are therefore expected to result in a complex spatial pattern, depending on altitude, latitude and longitude. Therefore, to study long-term variations of the ozone field, there is a need for long-term consistent time series with a good temporal and spatial coverage of the whole globe.

Passive satellite instruments are able to provide good continuous global coverage and can be classified as nadir-viewing and limb-viewing (including occultation) sounders (Hassler et al., 2014). For stratospheric studies the limb geometry is the preferred choice: as it provides relatively high vertical resolution. Several limb techniques have been developed over the last decades: in this paper we use data from limb scattering, limb emission and solar occultation instruments. The first type collects solar light scattered into the field of view of the instrument, the second one measures radiance emitted by atmospheric compounds in the infrared (IR) and microwave spectral region, whereas the latter one looks into the solar disk and measures radiance attenuated along the ray-path through the atmosphere. The latter technique enables measurements of atmospheric trace gases profiles with a higher precision with respect to the other two but with a sparser spatial sampling, since the observations are only made at sunset and sunrise. The use of shortwave limb scatter technique was for the first time successfully exploited by the NASA LORE/SOLSE (Limb Ozone Retrieval Experiment/Shuttle Ozone Limb Sounding Experiment) instrument launched in 1997. The Optical Spectrograph and Infrared Imager System (OSIRIS) launched in February 2001 (Llewellyn et al., 1997) and the SCanning Imaging Absorption spectroMeter for Atmospheric CHartography (SCIAMACHY), launched in March 2002 (Burrows et al., 1995; Gottwald and Bovensmann, 2010) followed on. At the end of 2011, a few months before the end of SCIAMACHY lifetime, the Ozone Mapping and Profiler Suite (OMPS) instrument was launched and it is still operational (Flynn et al., 2014). Stratospheric ozone profile is currently monitored by limb sounders like the aging OSIRIS and the Microwave Limb Sounder (MLS). In addition, solar occultation observations are done by the Canadian SCISAT (SCience SATellite), launched in 2004, and the Stratospheric Aerosol and Gas Experiment (SAGE) III on the international space station, which was launched in 2017.

In order to study the long-term changes in ozone vertical profiles and understand the impact of natural phenomena and anthropogenic activities on atmospheric ozone, single instrument time series are too short; several methodologies to consistently merge satellite data sets have been developed in the last years. In Harris et al. (2015), the authors considered several satellite data sets, merged them over the period 1979–2012 and examined separately the time spans before and after the peak in ODSs concentration at the end of '90s. The authors reported negative trends in the upper stratosphere of -5 % to -10 % per decade before 1998 a positive trend of 2 % after 1998 at mid-latitudes and 3 % in the tropics. They also stress different features visible in each single data set and the difficulty to establish the significance of trends in the latter period, requesting longer observational records, improvements in the consistency of single data sets, and more accurate data merging with uncertainties estimates. Steinbrecht et al. (2017) updated this work, using several available merged satellite and ground based data sets and focusing on 2000–2016 trends. A significant increase of ozone in the upper stratosphere was reported, with values of 2–2.5 % per decade at mid-latitudes and 1.5 % in the tropics. Sofieva et al. (2017) merged measurements from SAGE II with Ozone-cci and OMPS satellite data sets using deseasonalized anomalies of zonal monthly mean time series to study trends over the 1980–2016 period, applying a multilinear regression analysis. Before 1997 strong negative trends from -4 % to -8 % per decade were confirmed in the upper stratosphere. After 1997, the authors showed statistically significant trend at upper stratospheric



mid-latitudes reaching up to 2 % per decade. Ball et al. (2018) applied a method independent from the ozone turnaround point to compute trends and showed for the first time some evidence of a negative trend in lower stratospheric ozone below 60° latitude. The authors claimed that the lower stratospheric decrease offsets the observed recovery in the upper stratosphere, leading to an overall decline of the stratospheric ozone column. This analysis has recently been challenged by Chipperfield et al. (2018). Bourassa et al. (2018) presented an updated trend analysis merging SAGE II with OSIRIS time series till 2017, after a pointing drift in OSIRIS data was accounted for. The authors identified positive ozone trends post-1997 of about 1–3 % per decade above 25 km especially at mid-latitudes. In the lower stratosphere negative trends were found at all latitudes with significant values generally below 20 km.

Two other projects dealing with merging of satellite observations of several trace gas species are SWOOSH (Stratospheric Water and OzOne Satellite Homogenized) (Davis et al., 2016) and GOZCARDS (Global OZone Chemistry And Related trace gas Data records for the Stratosphere) (Froidevaux et al., 2015). The first study brought together satellite limb observations, providing several products such as water vapor and ozone mixing ratio profiles using different griddings on pressure levels starting from 1980. The second created time series of zonal monthly mean values of several trace gas species using NASA satellites. The LOTUS (Long-term Ozone Trends and Uncertainties in the Stratosphere, see <http://www.sparc-climate.org/activities/ozone-trends/>) project is focused on investigating uncertainties in ozone trends and homogenizing the merging procedures and the trend evaluations.

This paper describes a merged ozone data set created using limb measurements from SCIAMACHY and OMPS. The two data sets were generated at the University of Bremen by applying a retrieval algorithm, which uses the same radiative transfer model and spectroscopic databases and was individually optimized for SCIAMACHY and OMPS. The overarching scientific objective was to derive consistent ozone data sets that could be merged with the help of a transfer function; the latter being necessary because of the limited overlap period of the two instruments (2.5 months). The merged data set comprises monthly averaged ozone profiles. One of the highlights of this merged data set, in comparison with those reported in several previous studies, is that it is longitudinally resolved in steps of 5° latitude and 20° longitude. This enables us to investigate long-term ozone changes as a function of altitude, latitude, and longitude over the past 15 years (2003 to 2018). In addition, we perform a merging of the two time series also in terms of ozone number density values, without subtracting the seasonal cycle from each data set. In order to investigate ozone trends over even longer periods, we also include sparser ozone profiles retrieved from occultation measurements made by SAGE II. This SAGE-II/SCIAMACHY/OMPS merged data set is limited to zonal monthly mean anomalies. Section 2 of the paper describes the instruments, data sets, and methods to retrieve ozone profiles used in this study. Section 3 introduces the merging of SCIAMACHY and OMPS data sets using two approaches. Section 4 reports about the long-term ozone changes, both zonally averaged and longitudinally resolved as derived from the SCIAMACHY/OMPS merged data. Results are discussed and compared with previous studies in Sect. 4. Section 5 introduces the merging of SCIAMACHY and OMPS zonal mean anomalies with SAGE II and discusses long-term ozone trends over the pre- and post-1997 periods.



2 Instruments and data sets

The SCIAMACHY instrument was launched in 2002 on board the ENVISAT satellite platform and made scientific measurements from August 2002 until April 2012, when a failure in the platform-to-ground communication occurred. In the limb mode, SCIAMACHY observed the atmosphere in-flight direction and scanned horizontally, covering 960 km across-track in four steps, and vertically every 3.3 km. The instrument had a wide spectral coverage, collecting radiances in 8 channels spanning from 240 to 2380 nm, with a spectral resolution varying from 0.22 to 1.48 nm depending on the channel (for a detailed description of the instrument see Burrows et al., 1995; Gottwald and Bovensmann, 2010).

The OMPS instrument was launched at the end of 2011 on board the Suomi-NPP satellite platform (Flynn et al., 2014). The suite is composed of three instruments, only the Limb Profiler (LP) is taken into consideration for this work. The instrument looks backwards with respect to the flight velocity vector. It observes the whole atmospheric range simultaneously without scanning through three vertical slits, the central one aligned with the satellite ground track and the other two sideways, performing measurements horizontally separated by 4.25° at the tangent point. The instrument collects spectral radiance on a two-dimensional charged coupled device (CCD) through two apertures and at two integration times, to account for the wide dynamic range of the scattered radiance. The CCD pixels are then sampled to get a single picture of the atmospheric state and interpolated to obtain level 1 gridded data (L1G). OMPS-LP has a spectral coverage from 280 to 1000 nm with a spectral resolution increasing from 1 nm in the Ultraviolet (UV) region to 30 nm in the near-IR.

In Table 1 some details of the SCIAMACHY instrument are reported together with information about the OMPS-LP instrument for direct comparison.

Table 1. Main characteristics of SCIAMACHY and OMPS-LP instruments.

	SCIAMACHY	OMPS-LP
Data time series	08.2002–04.2012	02.2012–06.2018*
Spectral coverage [nm]	240–2300	280–1000
Spectral resolution [nm]	0.2–1.4	1–30
Instantaneous field of view [km]	2.6	1.5
Number of observations per orbit	~120	180 (each slit)

* used in this paper

In this study we consider version 3.5 of SCIAMACHY ozone profile retrieval and OMPS-LP version 2.0: both products were created at the University of Bremen using the SCIATRAN software package which includes a radiative transfer model and a retrieval algorithm (Rozanov et al., 2014). As discussed above and listed in Table 1, differences in terms of spectral coverage and resolution, observation method and radiance collection prevented a direct application of SCIAMACHY retrieval scheme to OMPS-LP. However for the retrieval of both data sets we used the same spectroscopic databases and the same initialization for atmospheric composition optical parameters. Both algorithms are based on a Tikhonov regularization scheme and use spectral windows in the UV Hartley-Huggins and in the visible Chappuis ozone band. The SCIAMACHY ozone profile



retrieval algorithm exploits the sun-normalized limb radiance measurements. For OMPS-LP, measurements of the solar spectral irradiance are not directly reported in V2.5 L1G data, so we normalize the radiance using upper-altitude tangent heights. In both cases we take into account in addition the absorption of NO_2 and O_4 , using the same cross sections but convolved to the respective resolution of the instruments. The weighting functions of the surface albedo are included in the fit procedure. The presence of a cloud in the instrument field of view is detected following the color index approach (Eichmann et al., 2016). Aerosol extinction profiles are retrieved for OMPS-LP using the methodology described in Rieger et al. (2018), whereas for SCIAMACHY climatological profiles are considered. SCIAMACHY profiles are reported from 8 to 64 km, OMPS-LP from 12 to 60 km. Only measurements from the central slit of the OMPS-LP instrument are used in this study; data from the lateral slits are planned to be used when the pointing knowledge issues, currently under investigation by NASA, are solved.

For more details about the University of Bremen OMPS-LP retrieval algorithm, implementation and validation readers are referred to Arosio et al. (2018); for a description of SCIAMACHY retrieval and the validation of the ozone profiles to Jia et al. (2015).

The MLS instrument was launched on board the Aura satellite and started scientific measurements in July 2004, observing the thermal emission from atmospheric trace gases in the millimeter/sub-millimeter spectral range. It scans the Earth limb 240 times per orbit providing retrievals of day- and nighttime profiles of several gases including ozone. For a detailed description of the MLS instrument readers are referred to Waters et al. (2006). In this paper, the version 4.2 of MLS level 2 (L2) data is used as a transfer function in the SCIAMACHY/OMPS-LP merging procedure. Quality flags and recommendations reported in Livesey et al. (2017) are taken into consideration throughout the study. Several studies, among which Hubert et al. (2016), investigated the stability of MLS ozone data set and found no significant drifts over the entire stratosphere.

SAGE II was launched in October 1984 on board the Earth Radiation Budget Satellite (ERBS) and operated until August 2005. The instrument had a sunphotometer collecting solar radiance attenuated by the atmosphere in seven wavelength ranges using the occultation geometry. For technical reasons, the observations of SAGE II are sparse in comparison to the other limb instruments: it could perform measurements only twice per orbit, resulting in 30 observations per day. The occultation geometry, however, yields a higher signal to noise ratio and the ozone profiles are provided with a vertical resolution of 0.5 km from cloud top to 60 km. For a more detailed overview of the instrument, readers are referred to McCormick (1987). In this study we use version 7.0 of SAGE II L2 data (Damadeo et al., 2013).

3 Merging the data sets

When merging different data sets, calibration discrepancies between the instruments as well as eventual drifts and jumps in the time series must be accounted for (Hubert et al., 2016). Since the overlap period of SCIAMACHY and OMPS missions is only about 2.5 months, too short for a reliable bias correction, we select a reference satellite data set to be used as an external transfer function. For this purpose, MLS was chosen because of the stability and reliability of its measurements, the extensive overlapping period with both instruments, its broad latitude coverage, and its dense sampling. In particular, we consider daytime MLS data from January 2005 until December 2016, taking only the latitude covered daily by OMPS-LP, to avoid inconsistency



between day and night measurements. The presence of the so-called South Atlantic Anomaly (SAA) is taken into consideration using for MLS and OMPS-LP the SAA flag provided in their respective L2 data and applying for SCIAMACHY a rectangular exclusion mask over the $[-70^\circ, -20^\circ]$ latitude and $[270^\circ, 360^\circ]$ longitude range. SCIAMACHY data from January 2003 till March 2012 are included (April is excluded because data for the first 8 days only are available), OMPS-LP data from February 2012 until June 2018 are used for merging. All profiles are provided in units of ozone number density on a geometric altitude grid. Volume mixing ratio ozone profiles from MLS on a pressure grid, are converted to geometric altitude vs. number density using pressures and temperatures from ECMWF ERA-Interim.

Different ways to bin the satellite data have been studied in order to find an optimal tradeoff between sufficient high spatial and temporal resolution of the merged product and the number of measurements in each bin, for the values to be representative. Two optimal sets of values are identified: a longitudinally resolved product, with monthly mean values on a 5° latitude and 20° longitude grid or a zonally averaged product with a temporal resolution of 10 days and a latitude resolution of 2.5° . In both cases we find about 100 profiles on average in each bin. The vertical grid used for the merged profiles has evenly spaced steps of 3.3 km, which corresponds to the typical SCIAMACHY vertical sampling: MLS and OMPS-LP profiles with higher vertical sampling are interpolated to this common grid.

In this paper we only describe the analysis of the longitudinally resolved ozone profile product. Figure 1 shows the number of measurements available for SCIAMACHY and OMPS-LP in each altitude and latitude bin as a function of time. These values have to be divided by 18, the number of longitudinal bins, to determine the number of measurements that contribute to each longitudinally resolved monthly mean value. The density of measurements increases in 2012, because OMPS-LP has a higher sampling per orbit than SCIAMACHY, as reported in Table 1.

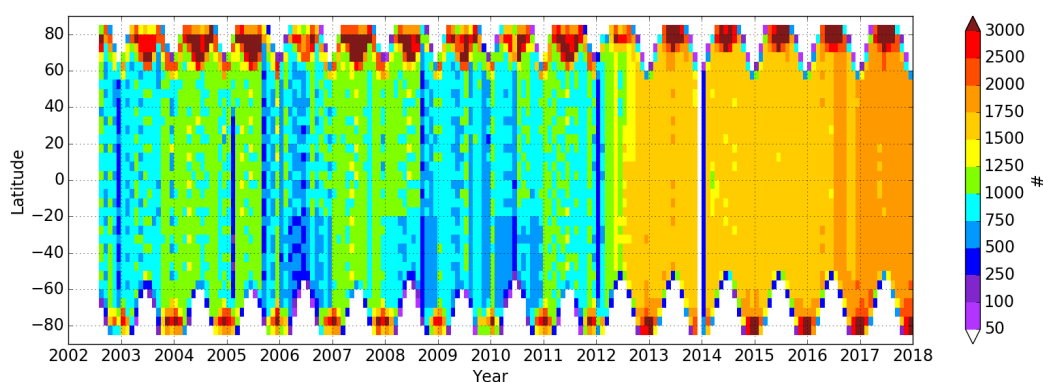


Figure 1. Number of SCIAMACHY and OMPS-LP observations as a function of time and latitude in each zonal monthly bin.

Two approaches are used to merge the SCIAMACHY and OMPS-LP data. In the first one, the so-called 'plain-debiasing' approach, the seasonal cycle (SC) of each instrument is kept: one data set is shifted with respect to the other, with the help of the transfer function, to remove the offset between the two. In the second one, the so-called 'anomalies' approach, which is similar to that used by Sofieva et al. (2017), the SC of the single instrument data set is determined and anomalies are calculated



independently for each data set before subtracting the offset between SCIAMACHY and OMPS-LP using the MLS anomalies as transfer function. We study the SCs of the three instruments to assess how well they agree and whether they need to be subtracted before merging. Figure 2 shows the SCs of the three instruments ozone profiles in number density [molec cm^{-3}] at different altitudes and latitudes.

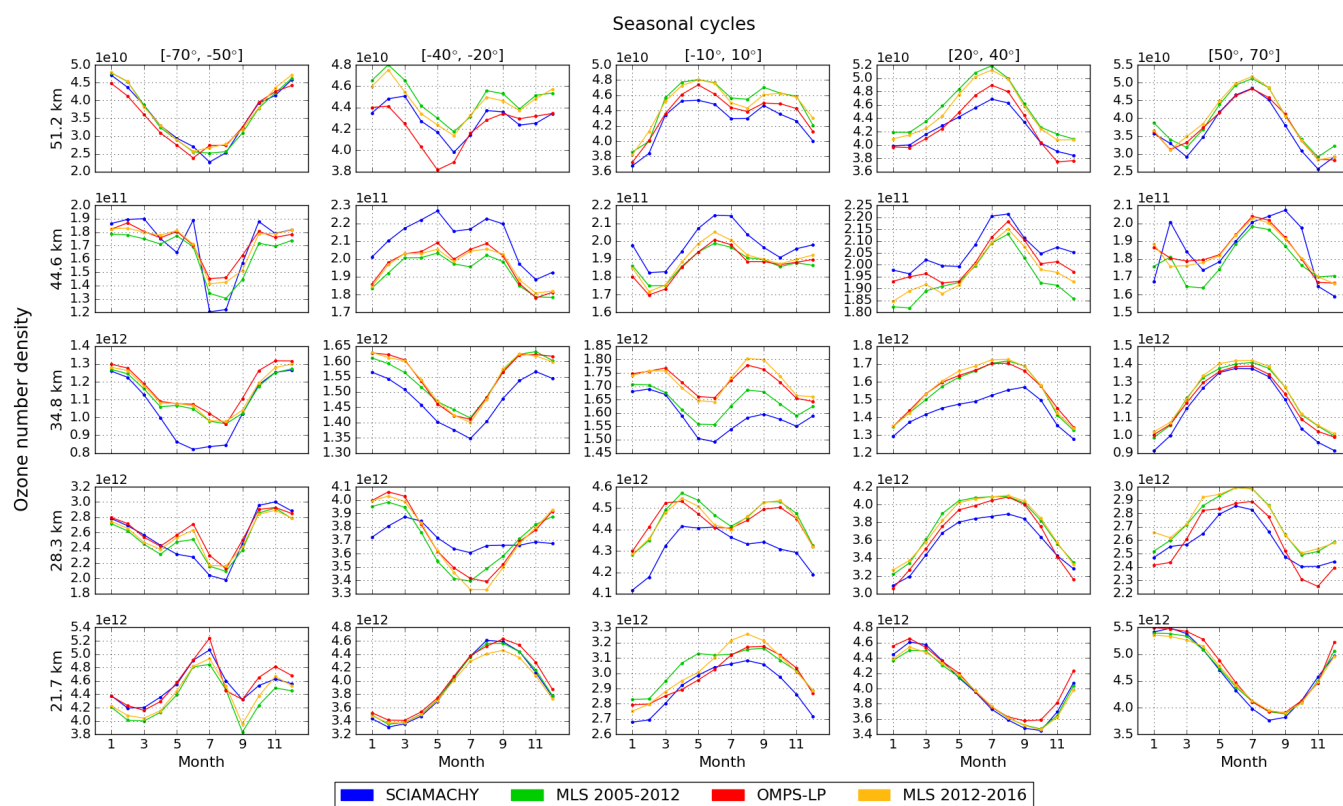


Figure 2. Seasonal cycle (SC) for the three instruments as a function of latitude and altitude, in terms of ozone number density [molec cm^{-3}]. MLS SC is plotted for the overlapping period with SCIAMACHY (2005–2012) and with OMPS-LP (2012–2016).

- 5 The SCIAMACHY ozone SC is compared to that from MLS profiles for the period 2005 to 2012, and the OMPS-LP ozone SC to that from MLS profiles for the period 2012 to 2016. At first glance, there is generally good agreement; however, discrepancies are visible in terms of the bias and the shape of the seasonal cycle between the instruments in some cases. Through the merging process biases will be subtracted, whereas the discrepancies in the shape of the SC are accounted for when calculating anomalies (subtraction of the SC). Two clear examples for these types of discrepancies are seen in the
- 10 latitude band $[-40^\circ, -20^\circ]$ at two altitudes (see Fig. 2):

1. at 34.8 km the SC of the three instruments show the same shape but different absolute values;
2. at 28.3 km SCIAMACHY SC has a significantly smaller amplitude with respect to the MLS and OMPS-LP.



Differences in the amplitudes are caused by the different vertical resolutions of the instruments and by the interpolation procedure we adopted; they are more pronounced at latitudes and altitudes where the transition between semi-annual to annual cycle occurs. In addition, we notice that MLS SC may vary within the instrument life time, as shown at 34.8 km in the tropics with change of up to 5–7 % between the two periods.

- 5 Since the SCs of the three instruments do not differ significantly except for few latitudes and altitudes, the first approach for merging SCIAMACHY and OMPS-LP time series consists in a plain debiasing of the two data sets with respect to MLS. The bias is defined for each latitude, longitude and altitude as follows:

$$BIAS_{SCIAMACHY} = mean(SCIAMACHY_{2005-2012}) - mean(MLS_{2005-2012}) \quad (1)$$

$$BIAS_{OMPS} = mean(OMPS_{2012-2016}) - mean(MLS_{2012-2016})$$

- 10 These biases are then applied to the OMPS-LP time series in such a way to conventionally keep the SCIAMACHY mean level as absolute reference as follows:

$$OMPS_{deb}(lat, lon, z) = OMPS(lat, lon, z) - BIAS_{OMPS}(lat, lon, z) + BIAS_{SCIA}(lat, lon, z) \quad (2)$$

- In this way, the offset between SCIAMACHY and OMPS-LP is accounted for with the help of MLS as transfer standard. The merging is then done by concatenating the two data sets and computing average values from SCIAMACHY and OMPS-LP over the two months of overlap, i.e. February–March 2012. We exclude all bins where the number of observations is lower than 10 or where the measurements from one of the instruments are not available. Figure 3 shows as a function of latitude for several altitudes relative differences between the merged data set and MLS time series (after the subtraction of its bias with respect to SCIAMACHY). Relative differences are within ± 10 % between 20 and 50 km and between 50° S and 50° N. Dashed vertical lines indicate the transitions between the two instruments. Over the SCIAMACHY measurement period, a small SC signature is observed, especially at 30–35 km at mid-latitudes and at 40–45 km at higher latitudes; these differences are already visible in Fig. 2. In the second half of the time series, less pronounced SC signatures are seen, particularly between 35 and 45 km. Below 20 km the differences increase rapidly showing strong seasonal pattern. Above 50 km, we notice a variation of the relative differences with time, suggesting the presence of drifts with respect to MLS within the time span of each instrument. Caution is therefore required in interpreting the computed trends above 50 km. Furthermore, at these altitudes diurnal variation of ozone have to be accounted for (Sakazaki et al., 2013), which was not done in this study. In addition, a technical change in the L1 processing of OMPS-LP UV data at the beginning of 2014 affects the OMPS-LP UV retrieval and leads to a jump above 50 km between the 2012–2013 period and the last three years of observations. Towards the polar regions, we notice increasing relative differences with respect to MLS, particularly above 40 km and below 25 km. In summary, we recommend the use of the 'plain-debiased' time series only within $\pm 60^\circ$ latitudes and the 20–50 km altitude range.

- 30 The second approach to merge data follows that from Sofieva et al. (2017) and comprises computing the deseasonalized anomalies from each data set and then debiasing them using MLS data. The SC for each month of the year, m , the anomalies,

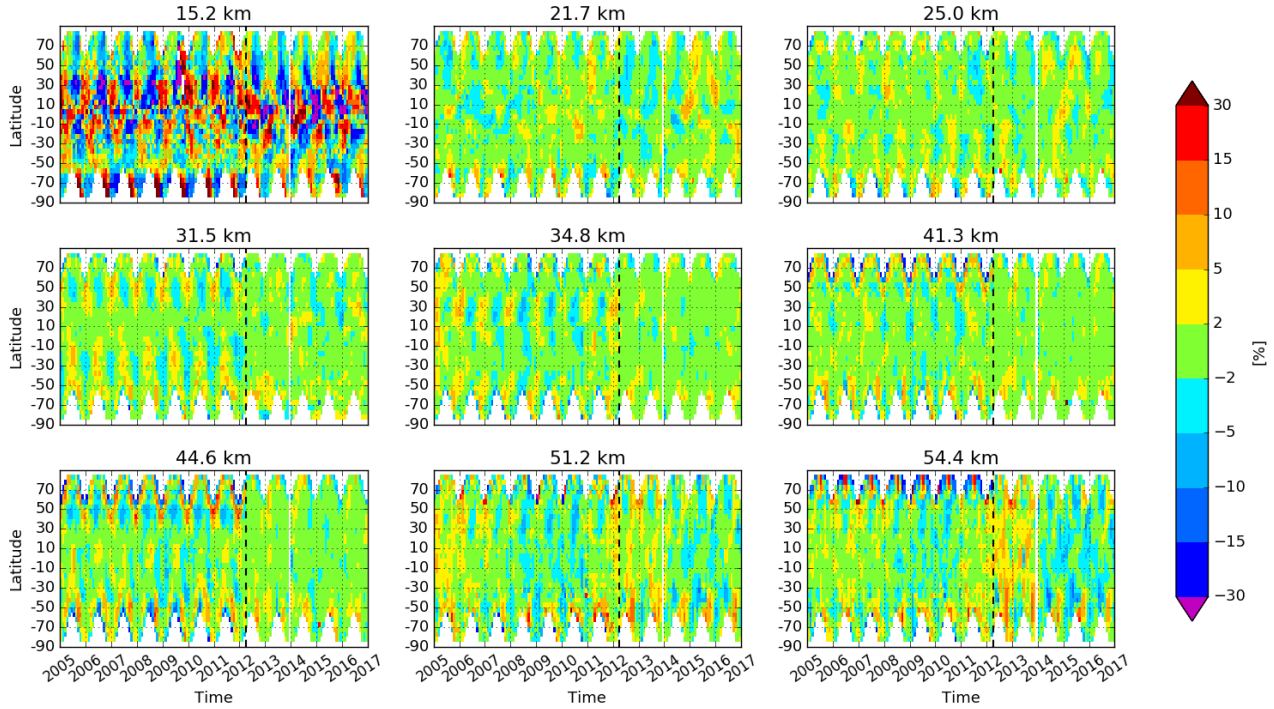


Figure 3. Relative differences of the debiased merged time series ('plain-debiasing' approach) with respect to MLS as a function of latitude for several altitudes. The vertical dashed lines indicate the transition between SCIAMACHY and OMPS-LP data sets.

Δ , and the respective uncertainties, $\sigma(t_m)$, are defined as:

$$SC_m = \frac{1}{N_m} \sum_{j=1}^{N_m} O_3(t_j) \quad (3)$$

$$\Delta(t_m) = \frac{O_3(t_m) - SC_m}{SC_m} \quad (4)$$

$$\sigma^2(t_m) = \frac{1}{N_m^2} \sum_{j=1}^{N_m} \sigma_{O_3}^2(t_j) \quad (5)$$

- 5 for SCIAMACHY, OMPS-LP and MLS, where N_m is the number of available monthly mean values $O_3(t_j)$ for the month of the year m in each time series and $\sigma_{O_3}(t_j)$ is the standard error of the mean for each monthly value respectively. The SC is computed for each instrument considering their complete time series. Then, the anomalies $\Delta(t_m)$ of SCIAMACHY and OMPS-LP are debiased using MLS anomalies as a transfer function as described by Eqs.(1) and (2). The merging is performed in the same way as done for the first approach. Figure 4 shows the differences of the merged anomalies with respect to the
- 10 MLS anomaly time series as a function of latitude for several altitudes. The differences are generally within $\pm 5\%$ also towards the polar regions between 20 and 50 km for both SCIAMACHY and OMPS-LP periods. Above 50 km, the presence of a drift



within the single data sets is again observed, whereas below 20 km the pattern becomes rather chaotic. We recommend the use of this data product within $\pm 70^\circ$ latitudes and over the 20–50 km altitude range.

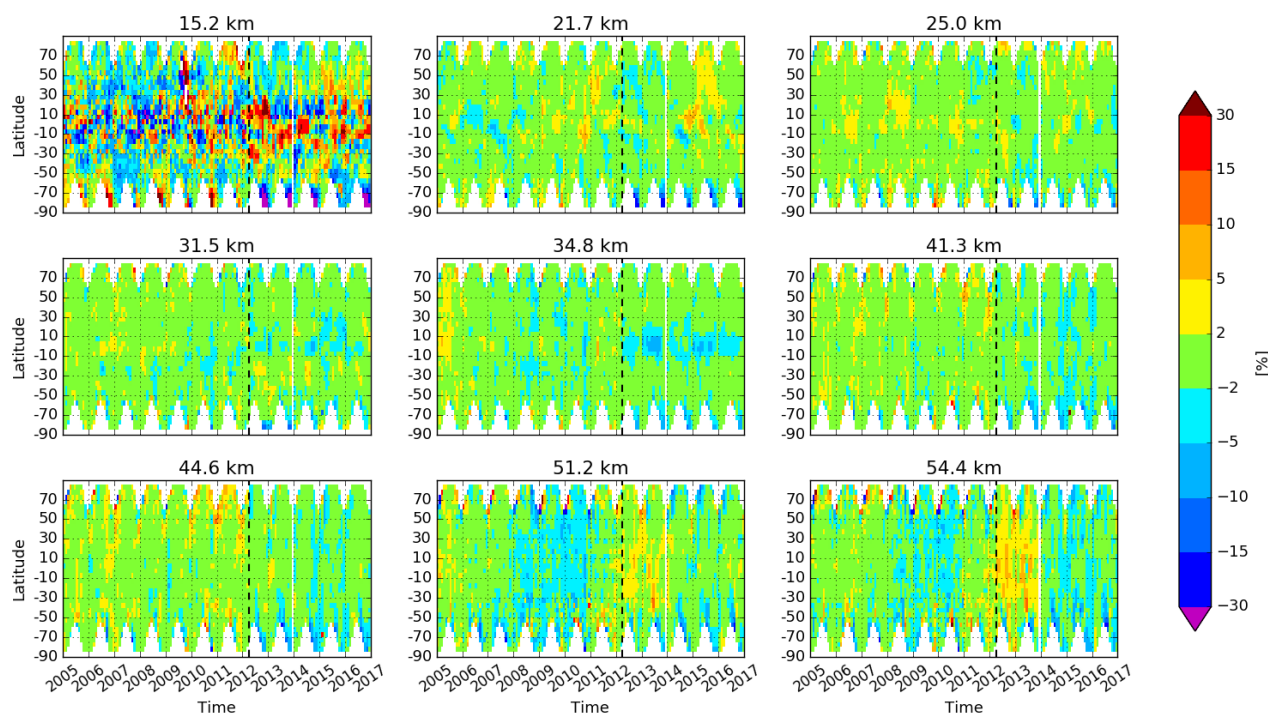


Figure 4. Differences of the merged relative anomaly time series with respect to MLS anomalies as a function of latitude at selected altitudes. The vertical dashed lines indicate the transition between SCIAMACHY and OMPS-LP data sets.

To check the consistency of the SCIAMACHY/OMPS-LP merged data set with respect to MLS, we compute the correlation coefficient and the drift for each latitude-altitude bin with respect to MLS over the period 2005–2016. The drift is computed as the linear change of the differences between the merged time series and MLS data, accounting also for seasonal variations as a sum of harmonic terms with periods of 6 and 12 months in the fit. Figure 5 shows in panel (a) the Pearson correlation coefficient as a function of altitude and latitude for the zonally averaged merged data set with respect to MLS, for the 'plain-debiased' merged data set (first approach). The correlation coefficient is high being typically above 0.8 between 20 and 50 km and within $\pm 70^\circ$ latitudes. A very similar result is obtained for the deseasonalized anomalies. Pearson correlation coefficient values are slightly lower because the strong SC removed in the anomalies contributes largely to the correlation. Panel (b) of Fig. 5 shows the drift of the merged data set with respect to MLS; dashed areas in this and the following figures indicate non-significant values, using a 95% confidence level. The drift is positive only in the tropical lower stratosphere and negative above 45 km but values are generally non-significant between 20 and 50 km: this means that the three debiased data sets (MLS and debiased SCIAMACHY and OMPS-LP) are consistent with each other over the 11 years of comparison and the long-term ozone changes



from the merged data set can be computed with high degree of confidence. Very similar results for the drift are obtained using anomalies time series. A plot of the longitude-resolved drift values is shown in the Supplements, Fig. S1.

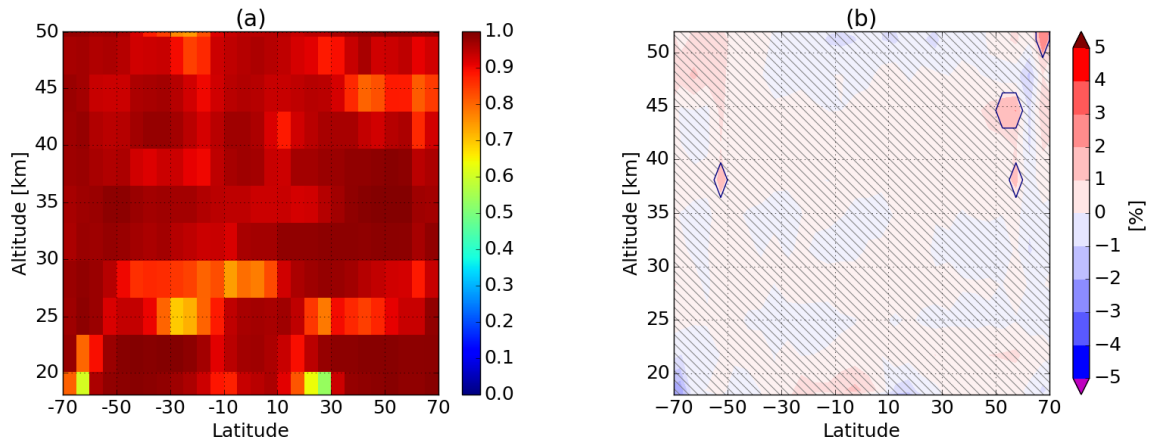


Figure 5. Panel (a): Pearson correlation coefficient of the merged debiased data set with respect to MLS time series over 2005–2016. Panel (b): drift of the merged debiased time series with respect to MLS; dashed areas identify regions where the drift is not statistically significant.

4 Trend analysis

4.1 Multivariate linear regression terms

- 5 To study recent long-term ozone variations we have selected the period January 2003–June 2018, consisting of 186 months. We follow a standard approach, applying an unweighted multilinear regression (MLR) model, accounting for several factors affecting ozone variability in the stratosphere. The weighting of each value by using the reciprocal of its corresponding squared standard deviation, i.e. $\sigma^2(t_m)$ in Eq. (5), has been tested but does not affect significantly the results. The autocorrelation of the data set with 1 month lag is accounted for, assuming the noise, N , to be an autoregressive process of the first order (Weatherhead
 10 et al., 1998). The following terms are considered in the MLR (Gebhardt et al., 2014):

$$O_3(t) = c_0 + c_1 t + \sum_{j=1}^2 \left(c_{2j} \sin\left(\frac{2\pi j t}{12}\right) + c_{3j} \cos\left(\frac{2\pi j t}{12}\right) \right) + QBO(t) + Solar(t) + ENSO(t) + N \quad (6)$$

or

$$O_3(t) = X\beta + N$$

- where t is the time in months and c_i are the regression coefficients, contained in the β vector. The t -th row of the X matrix
 15 contains the values of the fit terms for the selected t . The trend uncertainty and thus the significance of the linear trend values are computed from the covariance matrix of the regression coefficients; the trend is significant at the 95 % significance level if



the following condition is fulfilled (Tiao et al., 1990):

$$\left| \frac{c_1}{\sigma_{c_1}} \right| = 2 \quad (7)$$

All trends shown here are expressed in % per decade.

The linear term determined from Eq. (6) is the ozone trend at a given altitude, latitude and longitude. The harmonic terms with a period of 6 and 12 months are considered only for the plain-debiased merged data set to approximate the seasonal behavior. For the 50–60° N latitude band, the seasonal variability of ozone below 25 km is approximated by adding a term containing the eddy heat flux time series. The eddy heat flux is used as a proxy for the strength of the BDC (Weber et al., 2011). Instead of the harmonic terms the 2 months lagged eddy heat flux at 50 hPa from ERA-Interim is integrated over each year starting from October and used as a fit proxy (Gebhardt et al., 2014).

The Quasi Biennial Oscillation (QBO) is a quasi-periodic variation of the tropical wind direction in the tropical stratosphere: easterly and westerly wind regimes propagate downward with a variable period of approximately 28 months at a given altitude level. Even though it is a tropical phenomenon, the effects of this variable wind pattern on ozone are not confined to the tropical region: they extend to mid- and high-latitudes and are associated with the secondary meridional circulation (Baldwin et al., 2001). Several studies (Park et al., 2017) illustrated the effects of the QBO on ozone profiles as a function of altitude with two peaks in the ozone changes found at 20–27 km and at 30–38 km, showing opposite phase in the tropics and the in phase at mid-latitudes. In this study the influence of QBO is accounted for by considering the monthly average of the zonal wind components measured at 10 and 30 hPa by sondes launched at Singapore station (available at <http://www.geo.fu-berlin.de/en/met/ag/strat/produkte/qbo/index.html>) as a fit proxy. This combination of tropical zonal winds is used at all altitudes and latitudes as follows:

$$QBO(t) = c_{4a} QBO_{10hPa}(t) + c_{4b} QBO_{30hPa}(t) \quad (8)$$

The solar activity has a noticeable impact on ozone especially in the upper stratosphere as a consequence of e.g. the 11 year cycle and associated strong solar proton events. Several studies based on satellite data sets showed the presence of an in-phase solar cycle variation of 2–4 % in upper stratospheric ozone (e.g. Remsberg and Lingenfelser, 2010). The correlation is found to be positive and without time lag. As a proxy for the solar activity we consider Mg II index, which is the core-to-wing ratio derived from the Mg II doublet that is known to be highly correlated to solar irradiance variability from the UV to the extreme-UV (Snow et al., 2014). The composite Mg II data set we use was derived at the University of Bremen from the Global Ozone Monitoring Experiment (GOME), SCIAMACHY, GOME-2A and GOME-2B data (and available at <http://www.iup.uni-bremen.de/UVSAT/Datasets/mgii>). The solar proxy is then given by:

$$Solar(t) = c_5 MgII(t) \quad (9)$$

A further dynamical process impacting stratospheric ozone is the ENSO. This ocean-atmosphere coupled oscillation over the tropical eastern Pacific Ocean has been shown to impact the BDC and is responsible for temperature anomalies in the upper troposphere and lower stratosphere, leading to a longitudinally dependent modifications of ozone in this region (Randel et al.,



2009). We include the El Nino 3.4 index as a fit proxy for ozone variations in the lower stratosphere, which is based on sea surface temperature anomalies averaged from 5° S–5° N and 170°–120° W. In particular, we considered a proxy based on a combination of El Nino 3.4 index anomalies and its derivative, in order to account for the time lag between the ENSO proxy and its signature in the ozone time series, as follows:

$$5 \quad ENSO(t) = c_6[N_{34} + \frac{dN_{34}}{dt}\Delta(t)] \quad (10)$$

where Δ indicates the time lag in months. An iterative procedure is used to assess Δ . Starting from a time lag of 2 months the MLR is repeated, updating the time lag at each iteration until it approaches a fraction of a month. The final time lag is allowed to vary between 0 and 12 months. If it does not converge within 10 iteration or exceeds this range, the ENSO proxy is not used in the regression. ENSO is taken into consideration only in the tropical regions (20° S–20° N) and up to 25 km.

10 4.2 Zonally and longitudinally resolved long-term ozone variations

Figure 6 shows long-term ozone changes of zonally averaged ozone as a function of latitude and altitude calculated using the MLR model applied to the two versions of SCIAMACHY/OMPS-LP merged data sets. In panel (a) considering the anomalies data set and in panel (b) following the plain-debiasing approach. The longitudinally resolved trends are reported in the Supplements, Fig. S2. The general picture in the two panels is very similar, even though trend values in panel (b) are slightly larger

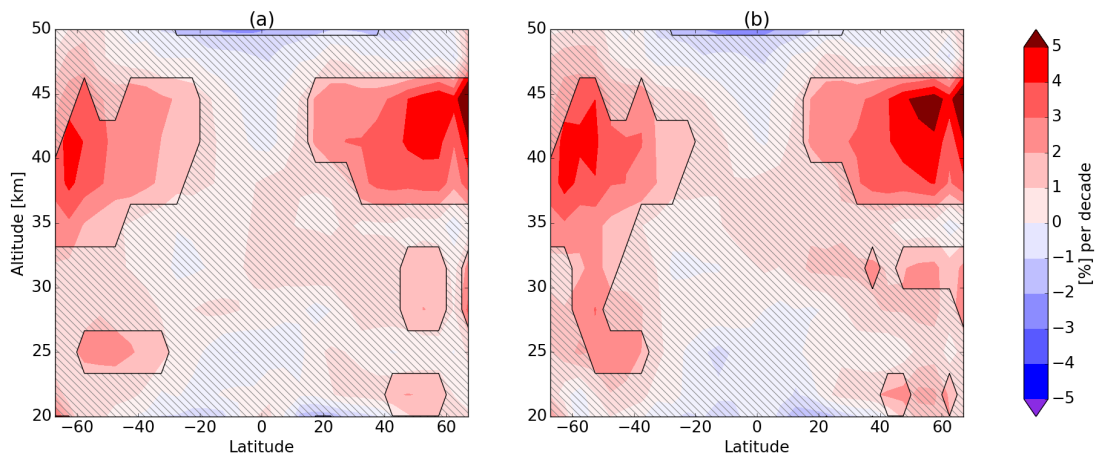


Figure 6. Zonal mean linear long-term ozone changes over the 2003–2018 period derived from the SCIAMACHY/OMPS-LP merged data sets: panel (a) shows the results using anomalies, panel (b) shows the results the plain-debiased data set. Dashed areas indicate non-significant trends.

15 compared to those in panel (a). Long-term changes are only statistically significant at mid-latitudes in the upper stratosphere. In this region the long term change is about 3–4 % per decade. This increase shows an asymmetry between the two hemispheres, with higher values at northern high-latitudes, also seen in other studies as (Bourassa et al., 2018). As discussed in Sect. 1, a



recovery of upper stratospheric ozone as a consequence of decreasing ODSs and increasing GHG emissions is expected and in agreement with recent studies (e.g. WMO (2014)). This is because at these altitudes the production of ozone results from the photolysis of ground molecular oxygen, $O_2(^3\Sigma_g^-)$ and the subsequent three body reaction of ground state oxygen atoms, $O(^3P)$, with $O_2(^1\Sigma_g^-)$ whereas ozone is lost by temperature-dependent catalytic odd oxygen cycles involving ClO_x , BrO_x , HO_x and NO_x . Above 48 km in the tropics the negative trends appear significant. As discussed in Sect. 3, these values have to be taken with caution as variations in the diurnal cycle are not accounted for. In addition, we tested the robustness of the trends by changing the starting point of the time series. When the time series starts from mid-2003 or beginning of 2004, the negative trend between 45 and 50 km is strongly reduced and is not significant anymore, whereas the positive trends get larger at mid-latitudes (of about 1%). This is a hint that this may be related to some instrumental issues at the beginning of the SCIAMACHY data set at these altitudes. In comparison with Ball et al. (2018), we do not identify extensively negative trends below 25 km in the tropics: at these altitudes in the $[-30^\circ, 30^\circ]$ latitude range negative trends are detected but are generally not significant. As can be seen in the Supplements, Fig. S2, only around 18–20 km in some longitude bins a statistically significant ozone decrease is detected.

Gebhardt et al. (2014) found over the 2002–2012 period positive trends in the upper stratosphere at mid-latitudes as well as in the tropics but also a strong negative trend in the tropics between 30 and 38 km up to -10 to -15 % per decade from a MLR analysis applied to an older version of SCIAMACHY data. Other studies have shown similar negative ozone changes in this altitude region. Kyrölä et al. (2013) found an ozone decrease of -2 to -4 % for 1997–2011 using merged data from SAGE II and GOMOS (Global Ozone Monitoring by Occultation of Stars), Eckert et al. (2014) found similar changes in 2002–2012 using MIPAS (Michelson Interferometer for Passive Atmospheric Sounding) observations and Nedoluha et al. (2015) showed a decrease of $-0.06 \text{ ppmv yr}^{-1}$ using HALOE (Halogen Occultation Experiment) and MLS measurements. Recently, Galytska et al. (July 2018) have studied this altitude range in the tropics using SCIAMACHY observations and TOMCAT chemical transport model (CTM). Model simulations reproduced the observed behavior in the period 2004–2012. They found anti-correlated changes in ozone and NO_2 from both SCIAMACHY observations and CTM calculations. They showed that these chemical changes are dynamically controlled by seasonal variations in the age of air (AoA) and thus in the vertical velocity of the BDC. In particular, the CTM showed a slow-down of the vertical transport during autumn months followed by a speed-up during winter months, causing changes in the residence time of N_2O and as a consequence in NO_2 and ozone profiles. When averaged over the whole year, AoA trends of different signs cancel out, resulting in no significant annual mean change, whereas the responses of N_2O and as a consequence NO_2 and ozone remain, due to a non-linear relation between chemistry and transport (Galytska et al., July 2018). This explains the annual mean trends in the SCIAMACHY ozone profiles observed in the tropical middle stratosphere until 2012. The model studies for the 2004–2018 period are ongoing.

Comparing the results presented in the above mentioned studies with Fig. 6 we notice that the negative trends found in the tropics around 35 km are not detected anymore and it is worth to have a look at the time series of ozone in this region, shown in Fig. 7, panel (a).

In this plot, the debiased time series is plotted along with the full regression fit and the linear trend term, considering both the whole time series and the 2003–2011 period. At 34.8 km we notice a decline in ozone until 2010–2012 (with a value close

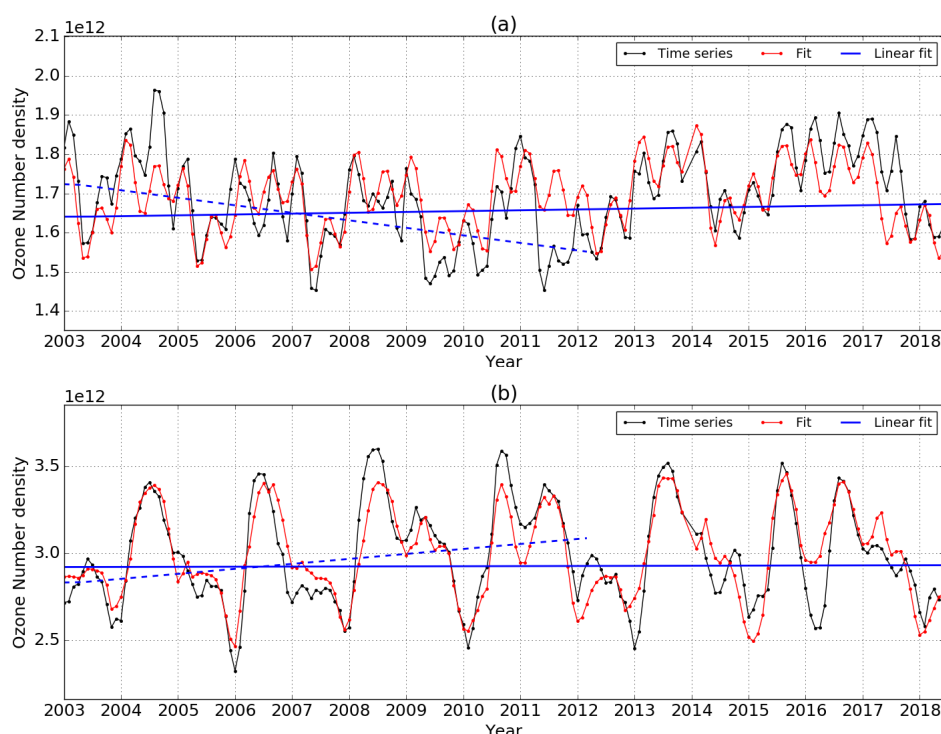


Figure 7. Merged number density time series of SCIAMACHY/OMPS-LP merged ozone (plain debiased) from 2003 to 2018 (in black) with MLR fit (in red) and linear trend term superimposed in blue (the dashed lines refer to the SCIAMACHY period until early 2012): in panel (a) at 34.8 km and in panel (b) at 21.7 km in the tropics, i.e. $[-5^{\circ}, 5^{\circ}]$ latitude bin.

to -10 % per decade), whereas after 2012 the ozone amount in this region leveled up to values recorded in mid-2000, resulting in nearly no change in ozone. This fact is enhanced by the anomalous QBO event that occurred in 2015–2016 (Newman et al., 2016), which led to higher ozone in the tropical region during 2016 (Tweedy et al., 2017). We have to notice that in this region MLS SC, as shown in Fig. 2, shows a particularly strong variation between SCIAMACHY and OMPS-LP periods: as
 5 a consequence, we found a strong sensitivity of the merging procedure for anomalies to the period over which MLS SC is computed.

In the lower tropical stratosphere, panel (b) of Fig. 7, the trend over 2003–2018 is also close to zero. However, looking at the period before and after 2011, we can notice that over the SCIAMACHY time a positive trend is present (7 % per decade), which was already reported by Gebhardt et al. (2014). Over the OMPS-LP period the tendency becomes flat or slightly negative,
 10 reducing the overall value of the trend.

Focusing on the altitudes where the ozone recovery is identified, Fig. 8 illustrates the latitudinal and longitudinal structure of the long-term ozone changes at 38 km. The longitudinal variability is remarkable, especially in the extra-tropical regions. For example, at northern mid- and high-latitudes ozone changes peak at above 5 % per decade over Canada but are near zero



over Siberia. Above Antarctica the trend is also positive, but a dedicated study focusing on ozone distribution during Antarctic spring is needed to assess the on-going ozone recovery in this region.

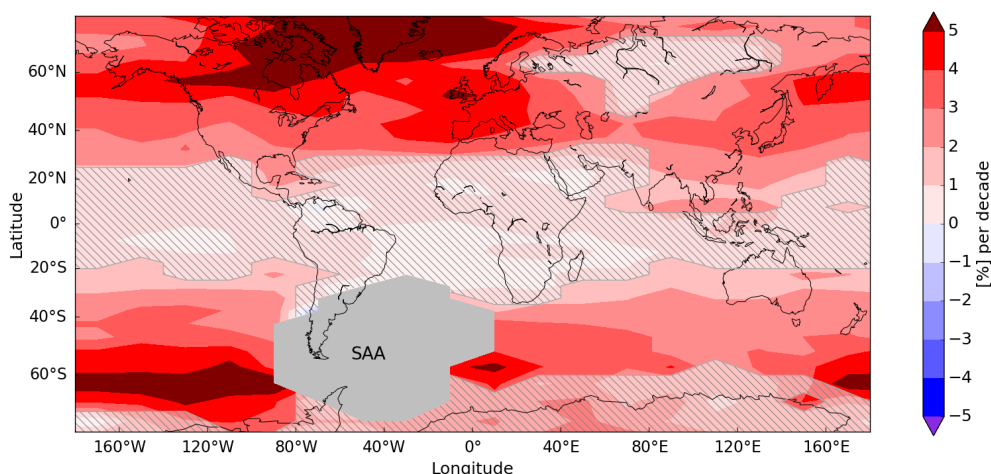


Figure 8. Longitudinally resolved ozone trends at 38 km in % per decade, computed over the 2003–2018 period from the SCIAMACHY/OMPS-LP merged data. Dashed areas indicate non-significant trends and the gray polygon labeled as SAA indicate the location of the South Atlantic Anomaly.

Kozubek et al. (2015) presented the structure of the BDC as a function of longitude and its impact on the ozone distribution, using reanalysis data. At 10 hPa a two-core structure of opposite meridional winds have been clearly identified by the authors at higher northern mid-latitudes, one centered over the Canadian and the other over the Asian sectors. Investigating trends in meridional wind at these heights, they found significant trends in these region, showing a weakening of the two-core structure after the ODS turn-around point in 1997. These changes in the dynamics of the stratosphere impact the ozone distribution in this region as well. This illustrates the limitations of the zonal mean approach to describe stratospheric dynamics and related ozone trends.

Similar maps showing the longitudinally resolved ozone field at 21 km and at 35 km are reported in the Supplements (Fig. S3 and S4, respectively).

5 Merging with SAGE II data set

The merging of SCIAMACHY and OMPS-LP data sets with SAGE II occultation observation is carried out considering zonal averaged monthly values, gridded every 10° latitude. This enables us to extend the SCIAMACHY/OMPS-LP data record back to 1984. The sparseness of SAGE II data prevents longitudinally resolved consideration or a finer latitude grid. The merging approach is based on anomalies: SAGE II, SCIAMACHY, MLS and OMPS-LP data sets are deseasonalised using their own SCs and then the offset with respect to SCIAMACHY is removed as done in Sect. 3. The debiasing of SAGE II time series



with respect to SCIAMACHY is done using the overlapping period between August 2002 and August 2005. In the merging procedure we reject altitude–latitude bins in two cases:

- if less than 10 measurements are available in the bin;
- if the distribution of SAGE II latitudes inside the bin is not representative for the latitude range, i.e. the mean SAGE II latitude and its standard deviation do not include the center latitude of the bin.

The same MLR model as discussed in Sect. 3 (without harmonic terms) is applied over four periods and the resulting trends are shown in Fig. 9, between 20 and 48 km and within $\pm 60^\circ$ latitudes. In the two upper panels of the figure the periods 1985–1997 and 1998–2018 are considered, assuming that in 1997 ODSs concentration peaked in the stratosphere. In agreement with the results presented for example by Sofieva et al. (2017) and Steinbrecht et al. (2017), we find negative trends above 30 km before 1997, reaching up to -6 % in the upper stratosphere at mid-latitudes. After 1998 the trends become positive and are significant at mid-latitudes above 35 km. We don't see in panel (b) negative trends in the tropics at 35 km. This results from the inclusion of the last 18 months of data. When we consider the time series until 2015 or 2016, a significant negative trend of about -2 % is detected in this region. In the two lower panels of Fig. 9 the focus is brought to the SCIAMACHY and OMPS-LP observation periods to see how short-term ozone changes depend on the periods selected in the MLR. In particular, the January 2004–December 2011 and February 2012–June 2018 periods are considered, as shown in panels (c) and (d), covering approximately an integer number of QBO cycles. Results in panel (c) can be compared with the trends reported in Gebhardt et al. (2014) and Galytska et al. (July 2018). Consistent with previous studies, we notice strong negative trends in the tropical middle stratosphere and positive significant trends in the southern lower stratosphere and in the upper stratosphere at northern mid-latitudes. The trends shown in panel (d) over the 2010–2018 period show an opposite picture with respect to panel (c) in the middle and lower stratosphere: positive changes in the tropics around 35 km and negative changes at southern mid-latitudes. Above 35 km extensively significant positive trends are found at all latitudes. These last two panels show how the long-term changes computed over the last 15 years are the result of complex changes in stratospheric dynamics, which occurred over shorter time scales, and the difficulty to disentangle atmospheric variability from long-term trends.

6 Conclusions

In this paper we described the approach and results of merging SCIAMACHY limb ozone profiles with OMPS-LP measurements. Monthly averaged data have been considered, binned every 5° latitude and 20° longitude, from January 2003 until June 2018. The merging has been achieved using MLS ozone profiles as a transfer function by following two approaches: in the first one ozone number density profiles are directly merged accounting for the bias between the two instruments independently at every latitude, longitude and altitude; in the second the SC of each instrument is firstly removed and debiased anomalies are then merged. Comparing the merged time series with MLS one, we found residual seasonal features using the first approach, preventing reliable results at high-latitudes. In the second approach, the merged and MLS anomalies showed discrepancies within ± 5 % up to the polar regions. A correlation coefficient above 0.8 with respect to MLS time series and no significant

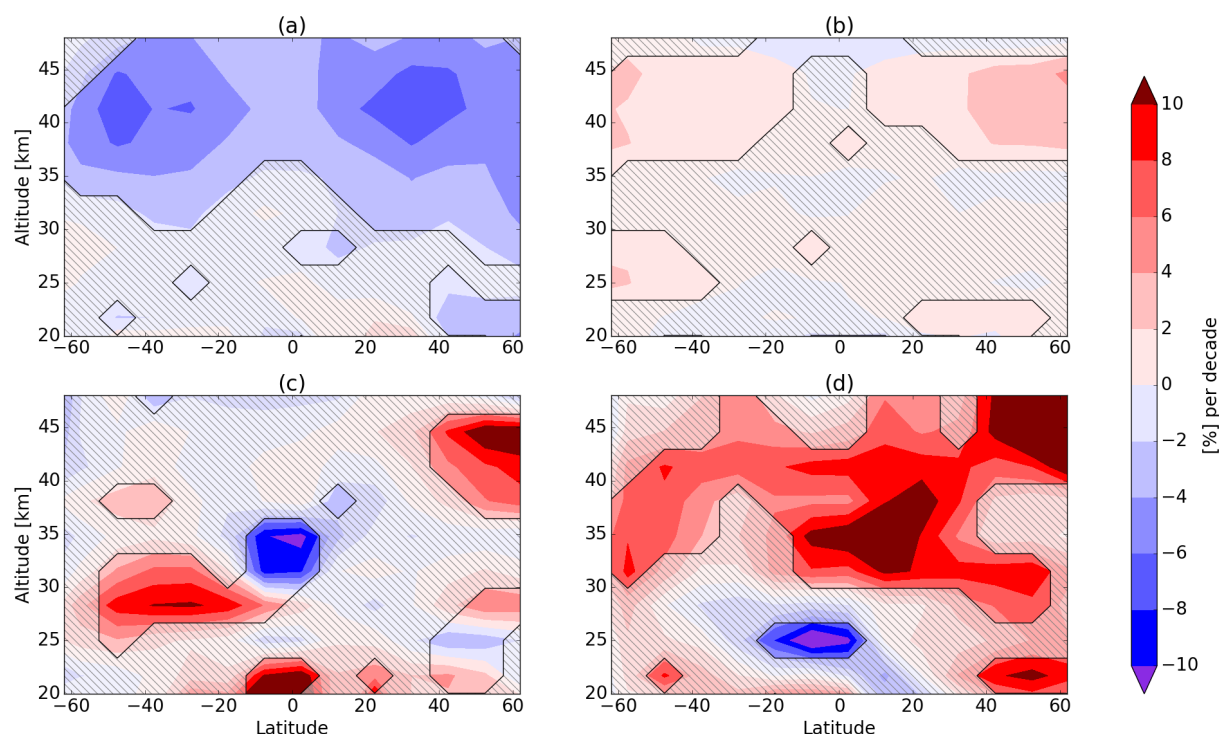


Figure 9. Zonal trends computed using the merged SAGE II, SCIAMACHY and OMPS-LP data set, in panel (a) over the 1985–1997 period, in panel (b) from 1997 to 2018, in panel (c) over 2002–2012 (SCIAMACHY observation period) and in panel (c) over 2012–2018 (OMPS-LP observation period). Dashed areas show non-significant trends.

drift between 20 and 50 km and between -70° and 70° latitude pointed out a good consistency of the merged data set. A MLR model has been applied to the merged data set to study long-term changes in the ozone profile, accounting for several factors affecting stratospheric ozone. Zonal mean trends showed a positive recovery of ozone at mid- and high-latitudes above 35 km, with significant positive changes of about 2–3 % per decade from 2013 until early 2018. Negative but non-significant trends were detected in the lower tropical stratosphere. Exploiting the high-spatial resolution of the data set, we also studied longitudinally resolved ozone changes, finding in the middle stratosphere a remarkable trend pattern that are indicative of changes in the BDC varying with longitudes at northern mid-latitudes. A comparison of our results with ozone long-term trends reported in previous studies showed a general consistency with regard to the apparent ozone recovery in the upper stratosphere. However, a change in the sign of the trends in the tropical region over the last 15 years was detected: the strong decrease around 35 km found for example by Gebhardt et al. (2014) over the SCIAMACHY period has vanished adding nearly five years of data. This is a consequence of several facts, such as the anomalous QBO event in 2015–2016, which led to positive ozone concentration anomalies in the tropics, and a possible change in the stratospheric dynamics with respect to the last decade. The merging procedure may affect the trends especially in regions where the SC of the instruments showed significant changes over



the considered period, for example around 35 km in the tropics. The merging of monthly zonal mean anomalies of SAGE II with SCIAMACHY and OMPS-LP data sets was performed to facilitate the study of zonal trends in particular over the periods 1985–1997 and 1998–2018. We obtained results in agreement with previous studies: decreasing trends up to -6 % per decade at mid-latitudes in the upper stratosphere before the ODSs turnaround point and an upper stratospheric recovery of about 3 % per decade after 1997, as a result of the implementation of measures agreed in the Montreal Protocol and its Amendments. A model study is planned to improve our understanding of the dynamical impact on the ozone trends in the tropical region over the last 15 years and the variations in ozone concentration over the SCIAMACHY and OMPS-LP periods.

7 Data availability

Our results and data sets are available upon request to the first two authors.

- 10 *Author contributions.* CA provided OMPS-LP data set, performed the merging of the time series, developed the procedure to compute trends and wrote the paper. AR supervised and guided the merging and the computation of the trends, provided SCIAMACHY data set and the tools for the MLR model and reviewed the manuscript. EM provided stratospheric aerosol data for OMPS-LP retrieval and revised of the manuscript. MW contributed with the fit proxies for the MLR, with the revision of the manuscript and guided SAGE II data handling. JPB initiated and proposed the research and led the project, he contributed to the data analysis, the establishment of the scientific outcomes and
- 15 the preparation of the manuscript.

Competing interests. The authors declare that they have no conflict of interest

Acknowledgements. This work was partially funded by ESA within the Ozone CCI project and was supported by the University and State of Bremen. We would like to acknowledge the NASA team for providing data and support. Part of the data processing has been done at the German HLRN (High Performance Computer Center North).



References

- Arosio, C., Rozanov, A., Malinina, E., Eichmann, K.-U., von Clarmann, T., and Burrows, J. P.: Retrieval of ozone profiles from OMPS limb scattering observations, *Atmospheric Measurement Techniques*, 11, 2135–2149, doi:10.5194/amt-11-2135-2018, <https://www.atmos-meas-tech.net/11/2135/2018/>, 2018.
- 5 Baldwin, M., Gray, L., Dunkerton, T., Hamilton, K., Haynes, P., Randel, W., Holton, J., Alexander, M., Hirota, I., Horinouchi, T., et al.: The quasi-biennial oscillation, *Reviews of Geophysics*, 39, 179–229, 2001.
- Ball, W. T., Alsing, J., Mortlock, D. J., Staehelin, J., Haigh, J. D., Peter, T., Tummon, F., Stübi, R., Stenke, A., Anderson, J., et al.: Evidence for a continuous decline in lower stratospheric ozone offsetting ozone layer recovery, *Atmospheric Chemistry and Physics*, 18, 1379–1394, 2018.
- 10 Bourassa, A. E., Roth, C. Z., Zawada, D. J., Rieger, L. A., McLinden, C. A., and Degenstein, D. A.: Drift-corrected Odin-OSIRIS ozone product: algorithm and updated stratospheric ozone trends, *Atmospheric Measurement Techniques*, 11, 489–498, doi:10.5194/amt-11-489-2018, <https://www.atmos-meas-tech.net/11/489/2018/>, 2018.
- Burrows, J., Hölzle, E., Goede, A., Visser, H., and Fricke, W.: SCIAMACHY—Scanning imaging absorption spectrometer for atmospheric cartography, *Acta Astronautica*, 35, 445–451, 1995.
- 15 Chipperfield, M. P., Dhomse, S., Hossaini, R., Feng, W., Santee, M. L., Weber, M., Burrows, J. P., Wild, J. D., Loyola, D., and Coldewey-Egbers, M.: On the Cause of Recent Variations in Lower Stratospheric Ozone, *Geophysical Research Letters*, 45, 5718–5726, 2018.
- Damadeo, R., Zawodny, J., Thomason, L., and Iyer, N.: SAGE version 7.0 algorithm: application to SAGE II, *Atmospheric Measurement Techniques*, 6, 3539–3561, 2013.
- Davis, S. M., Rosenlof, K. H., Hassler, B., Hurst, D. F., Read, W. G., Vömel, H., Selkirk, H., Fujiwara, M., and Damadeo, R.: The Strato-
- 20 spheric Water and Ozone Satellite Homogenized (SWOOSH) database: A long-term database for climate studies, *Earth System Science Data*, 8, 461, 2016.
- Eckert, E., Clarmann, T. v., Kiefer, M., Stiller, G., Lossow, S., Glatthor, N., Degenstein, D., Froidevaux, L., Godin-Beekmann, S., Leblanc, T., et al.: Drift-corrected trends and periodic variations in MIPAS IMK/IAA ozone measurements, *Atmospheric Chemistry and Physics*, 14, 2571–2589, 2014.
- 25 Eichmann, K.-U., Lelli, L., von Savigny, C., Sembhi, H., and Burrows, J. P.: Global cloud top height retrieval using SCIAMACHY limb spectra: model studies and first results, *Atmospheric Measurement Techniques*, 9, 793–815, doi:10.5194/amt-9-793-2016, <https://www.atmos-meas-tech.net/9/793/2016/>, 2016.
- Flynn, L., Long, C., Wu, X., Evans, R., Beck, C., Petropavlovskikh, I., McConville, G., Yu, W., Zhang, Z., Niu, J., et al.: Performance of the ozone mapping and profiler suite (OMPS) products, *Journal of Geophysical Research: Atmospheres*, 119, 6181–6195, 2014.
- 30 Froidevaux, L., Anderson, J., Wang, H.-J., Fuller, R. A., Schwartz, M. J., Santee, M. L., Livesey, N. J., Pumphrey, H. C., Bernath, P. F., Russell III, J. M., and McCormick, M. P.: Global OZone Chemistry And Related trace gas Data records for the Stratosphere (GOZ-CARDS): methodology and sample results with a focus on HCl, H₂O, and O₃, *Atmospheric Chemistry and Physics*, 15, 10471–10507, doi:10.5194/acp-15-10471-2015, <https://www.atmos-chem-phys.net/15/10471/2015/>, 2015.
- Galytska, E., Rozanov, A., Chipperfield, M., Dhomse, S., Weber, M., Arosio, C., Feng, W., and Burrows, J.: Dynamically controlled ozone
- 35 decline in the tropical mid-stratosphere observed by SCIAMACHY [Discussion paper], Submitted to: *Atmospheric Chemistry and Physics*, July 2018.



- Garcia, R. R. and Randel, W. J.: Acceleration of the Brewer–Dobson circulation due to increases in greenhouse gases, *Journal of the Atmospheric Sciences*, 65, 2731–2739, 2008.
- Gebhardt, C., Rozanov, A., Hommel, R., Weber, M., Bovensmann, H., Burrows, J., Degenstein, D., Froidevaux, L., and Thompson, A.: Stratospheric ozone trends and variability as seen by SCIAMACHY from 2002 to 2012, *Atmospheric Chemistry and Physics*, 14, 831–846, 2014.
- Gottwald, M. and Bovensmann, H.: SCIAMACHY-Exploring the changing Earth's Atmosphere, Springer Science & Business Media, 2010.
- Groves, K. and Tuck, A.: Simultaneous effects of CO₂ and chlorofluoromethanes on stratospheric ozone, *Nature*, 280, 127, 1979.
- Groves, K., Mattingly, S., and Tuck, A.: Increased atmospheric carbon dioxide and stratospheric ozone, *Nature*, 273, 711, 1978.
- Harris, N. R. P., Hassler, B., Tummon, F., Bodeker, G. E., Hubert, D., Petropavlovskikh, I., Steinbrecht, W., Anderson, J., Bhartia, P. K., Boone, C. D., Bourassa, A., Davis, S. M., Degenstein, D., Delcloo, A., Frith, S. M., Froidevaux, L., Godin-Beekmann, S., Jones, N., Kurylo, M. J., Kyrölä, E., Laine, M., Leblanc, S. T., Lambert, J.-C., Liley, B., Mahieu, E., Maycock, A., de Mazière, M., Parrish, A., Querel, R., Rosenlof, K. H., Roth, C., Sioris, C., Staehelin, J., Stolarski, R. S., Stübi, R., Tamminen, J., Vigouroux, C., Walker, K. A., Wang, H. J., Wild, J., and Zawodny, J. M.: Past changes in the vertical distribution of ozone – Part 3: Analysis and interpretation of trends, *Atmospheric Chemistry and Physics*, 15, 9965–9982, doi:10.5194/acp-15-9965-2015, <https://www.atmos-chem-phys.net/15/9965/2015/>, 2015.
- Hassler, B., Petropavlovskikh, I., Staehelin, J., August, T., Bhartia, P., Clerbaux, C., Degenstein, D., Mazière, M. D., Dinelli, B., Dudhia, A., et al.: Past Changes in the Vertical Distribution of Ozone Part 1: Measurement Techniques, Uncertainties and Availability, 2014.
- Hubert, D., Lambert, J.-C., Verhoelst, T., Granville, J., Keppens, A., Baray, J.-L., Cortesi, U., Degenstein, D., Froidevaux, L., Godin-Beekmann, S., et al.: Ground-based assessment of the bias and long-term stability of fourteen limb and occultation ozone profile data records, *Atmospheric measurement techniques*, 9, 2497, 2016.
- Jia, J., Rozanov, A., Ladstätter-Weissenmayer, A., and Burrows, J.: Global validation of SCIAMACHY limb ozone data (versions 2.9 and 3.0, IUP Bremen) using ozonesonde measurements, *Atmospheric Measurement Techniques*, 8, 3369–3383, 2015.
- Kozubek, M., Krizan, P., and Lastovicka, J.: Northern Hemisphere stratospheric winds in higher midlatitudes: longitudinal distribution and long-term trends, *Atmospheric Chemistry and Physics*, 15, 2203–2213, doi:10.5194/acp-15-2203-2015, <https://www.atmos-chem-phys.net/15/2203/2015/>, 2015.
- Kyrölä, E., Laine, M., Sofieva, V., Tamminen, J., Päiväranta, S.-M., Tukiainen, S., Zawodny, J., and Thomason, L.: Combined SAGE II–GOMOS ozone profile data set for 1984–2011 and trend analysis of the vertical distribution of ozone, *Atmospheric Chemistry and Physics*, 13, 10 645–10 658, 2013.
- Livesey, N., Read, W., Wagner, P., Froidevaux, L., Lambert, A., Manney, G. L., Millan Valle, L. F., Pumphrey, H. C., Santee, M. L., Schwartz, M. J., Wang, S., Fuller, R. A., Jarnot, R. F., Knosp, B. W., and Martinez, E.: Version 4.2x Level 2 data quality and description document, 2017.
- Llewellyn, E., Degenstein, D., McDade, I., Gattinger, R., King, R., Buckingham, R., Richardson, E., Murtagh, D., Evans, W., Solheim, B., et al.: Osiris—An Application of Tomography for Absorbed Emissions in Remote Sensing, in: *Applications of Photonic Technology 2*, pp. 627–632, Springer, 1997.
- McCormick, M.: SAGE II: an overview, *Advances in Space Research*, 7, 219–226, 1987.
- Morgenstern, O., Stone, K. A., Schofield, R., Akiyoshi, H., Yamashita, Y., Kinnison, D. E., Garcia, R. R., Sudo, K., Plummer, D. A., Scinocca, J., Oman, L. D., Manyin, M. E., Zeng, G., Rozanov, E., Stenke, A., Revell, L. E., Pitari, G., Mancini, E., Di Genova, G., Visioni, D., Dhomse, S. S., and Chipperfield, M. P.: Ozone sensitivity to varying greenhouse gases and ozone-depleting substances in CCMI-1



- simulations, *Atmospheric Chemistry and Physics*, 18, 1091–1114, doi:10.5194/acp-18-1091-2018, <https://www.atmos-chem-phys.net/18/1091/2018/>, 2018.
- Nedoluha, G., Siskind, D., Lambert, A., and Boone, C.: The decrease in mid-stratospheric tropical ozone since 1991, *Atmospheric Chemistry and Physics*, 15, 4215–4224, 2015.
- 5 Newman, P., Coy, L., Pawson, S., and Lait, L.: The anomalous change in the QBO in 2015–2016, *Geophysical Research Letters*, 43, 8791–8797, 2016.
- Park, M., Randel, W., Kinnison, D., Bourassa, A., Degenstein, D., Roth, C., McLinden, C., Sioris, C., Livesey, N., and Santee, M.: Variability of Stratospheric Reactive Nitrogen and Ozone Related to the QBO, *Journal of Geophysical Research: Atmospheres*, 122, 2017.
- Portmann, R., Daniel, J., and Ravishankara, A.: Stratospheric ozone depletion due to nitrous oxide: influences of other gases, *Phil. Trans. R. Soc. B*, 367, 1256–1264, 2012.
- 10 Randel, W. J., Garcia, R. R., Calvo, N., and Marsh, D.: ENSO influence on zonal mean temperature and ozone in the tropical lower stratosphere, *Geophysical Research Letters*, 36, 2009.
- Ravishankara, A., Daniel, J. S., and Portmann, R. W.: Nitrous oxide (N₂O): the dominant ozone-depleting substance emitted in the 21st century, *science*, 326, 123–125, 2009.
- 15 Remsberg, E. and Lingenfelser, G.: Analysis of SAGE II ozone of the middle and upper stratosphere for its response to a decadal-scale forcing, *Atmospheric Chemistry and Physics*, 10, 11 779–11 790, 2010.
- Rieger, L. A., Malinina, E. P., Rozanov, A. V., Burrows, J. P., Bourassa, A. E., and Degenstein, D. A.: A study of the approaches used to retrieve aerosol extinction, as applied to limb observations made by OSIRIS and SCIAMACHY, *Atmospheric Measurement Techniques*, 11, 3433–3445, doi:10.5194/amt-11-3433-2018, <https://www.atmos-meas-tech.net/11/3433/2018/>, 2018.
- 20 Rozanov, V., Rozanov, A., Kokhanovsky, A., and Burrows, J.: Radiative transfer through terrestrial atmosphere and ocean: software package SCIATRAN, *Journal of Quantitative Spectroscopy and Radiative Transfer*, 133, 13–71, 2014.
- Sakazaki, T., Fujiwara, M., Mitsuda, C., Imai, K., Manago, N., Naito, Y., Nakamura, T., Akiyoshi, H., Kinnison, D., Sano, T., et al.: Diurnal ozone variations in the stratosphere revealed in observations from the Superconducting Submillimeter-Wave Limb-Emission Sounder (SMILES) on board the International Space Station (ISS), *Journal of Geophysical Research: Atmospheres*, 118, 2991–3006, 2013.
- 25 Snow, M., Weber, M., Machol, J., Viereck, R., and Richard, E.: Comparison of Magnesium II core-to-wing ratio observations during solar minimum 23/24, *Journal of Space Weather and Space Climate*, 4, A04, 2014.
- Sofieva, V. F., Kyrölä, E., Laine, M., Tamminen, J., Degenstein, D., Bourassa, A., Roth, C., Zawada, D., Weber, M., Rozanov, A., et al.: Merged SAGE II, Ozone_cci and OMPS ozone profile dataset and evaluation of ozone trends in the stratosphere, *Atmospheric Chemistry and Physics*, 17, 12 533–12 552, 2017.
- 30 Steinbrecht, W., Froidevaux, L., Fuller, R., Wang, R., Anderson, J., Roth, C., Bourassa, A., Degenstein, D., Damadeo, R., Zawodny, J., Frith, S., McPeters, R., Bhartia, P., Wild, J., Long, C., Davis, S., Rosenlof, K., Sofieva, V., Walker, K., Rappoe, N., Rozanov, A., Weber, M., Laeng, A., von Clarmann, T., Stiller, G., Kramarova, N., Godin-Beekmann, S., Leblanc, T., Querel, R., Swart, D., Boyd, I., Hocke, K., Kämpfer, N., Maillard Barras, E., Moreira, L., Nedoluha, G., Vigouroux, C., Blumenstock, T., Schneider, M., García, O., Jones, N., Mahieu, E., Smale, D., Kotkamp, M., Robinson, J., Petropavlovskikh, I., Harris, N., Hassler, B., Hubert, D., and Tummon, F.: An update on ozone profile trends for the period 2000 to 2016, *Atmospheric Chemistry and Physics*, 17, 10 675–10 690, doi:10.5194/acp-17-10675-2017, <https://www.atmos-chem-phys.net/17/10675/2017/>, 2017.
- 35



- Tiao, G., Reinsel, G., Xu, D., Pedrick, J., Zhu, X., Miller, A., DeLuisi, J., Mateer, C., and Wuebbles, D.: Effects of autocorrelation and temporal sampling schemes on estimates of trend and spatial correlation, *Journal of Geophysical Research: Atmospheres*, 95, 20 507–20 517, 1990.
- 5 Tweedy, O. V., Kramarova, N. A., Strahan, S. E., Newman, P. A., Coy, L., Randel, W. J., Park, M., Waugh, D. W., and Frith, S. M.: Response of trace gases to the disrupted 2015–2016 quasi-biennial oscillation, *Atmospheric Chemistry and Physics*, 17, 6813–6823, 2017.
- Waters, J. W., Froidevaux, L., Harwood, R. S., Jarnot, R. F., Pickett, H. M., Read, W. G., Siegel, P. H., Cofield, R. E., Filipiak, M. J., Flower, D. A., et al.: The earth observing system microwave limb sounder (EOS MLS) on the Aura satellite, *IEEE Transactions on Geoscience and Remote Sensing*, 44, 1075–1092, 2006.
- 10 Waugh, D., Oman, L., Kawa, S., Stolarski, R., Pawson, S., Douglass, A., Newman, P., and Nielsen, J.: Impacts of climate change on stratospheric ozone recovery, *Geophysical Research Letters*, 36, 2009.
- Weatherhead, E. C., Reinsel, G. C., Tiao, G. C., Meng, X.-L., Choi, D., Cheang, W.-K., Keller, T., DeLuisi, J., Wuebbles, D. J., Kerr, J. B., et al.: Factors affecting the detection of trends: Statistical considerations and applications to environmental data, *Journal of Geophysical Research: Atmospheres*, 103, 17 149–17 161, 1998.
- 15 Weber, M., Dikty, S., Burrows, J. P., Garny, H., Dameris, M., Kubin, A., Abalichin, J., and Langematz, U.: The Brewer-Dobson circulation and total ozone from seasonal to decadal time scales, *Atmospheric Chemistry and Physics*, 11, 11 221–11 235, 2011.
- WMO: Scientific Assessment of Ozone Depletion 2014, Global Ozone Research and Monitoring Project Report 55, World Meteorological Organization, <https://www.esrl.noaa.gov/csd/assessments/ozone/2014/chapters/2014OzoneAssessment.pdf>, 2014.